

Article

# Genetic Algorithm-Based Optimization Methodology of Bézier Curves to Generate a DCI Microscale-Model

Jesus A. Basurto-Hurtado <sup>1</sup>, Roque A. Osornio-Rios <sup>1</sup> , Arturo Y. Jaen-Cuellar <sup>1</sup>, Aurelio Dominguez-Gonzalez <sup>2</sup> and L. A. Morales-Hernandez <sup>1,\*</sup> 

<sup>1</sup> Mechatronics CA, Faculty of Engineering, Autonomous University of Queretaro, Campus San Juan del Rio, Rio Moctezuma 249, Col. San Cayetano, San Juan del Rio, Queretaro 76805, Mexico; jbasurto@hspdigital.org (J.A.B.-H.); raosornio@hspdigital.org (R.A.O.-R.); ayjaen@hspdigital.org (A.Y.J.-C.)

<sup>2</sup> Faculty of Engineering, Autonomous University of Queretaro, Cerro de las Campanas S/N, Col. Las Campanas, Santiago de Queretaro, Queretaro 76010, Mexico; auredgz@uaq.mx

\* Correspondence: lamorales@hspdigital.org; Tel.: +52-427-274-1244

Received: 23 October 2017; Accepted: 24 November 2017; Published: 28 November 2017

**Abstract:** The aim of this article is to develop a methodology that is capable of generating micro-scale models of Ductile Cast Irons, which have the particular characteristic to preserve the smoothness of the graphite nodules contours that are lost by discretization errors when the contours are extracted using image processing. The proposed methodology uses image processing to extract the graphite nodule contours and a genetic algorithm-based optimization strategy to select the optimal degree of the Bézier curve that best approximate each graphite nodule contour. To validate the proposed methodology, a Finite Element Analysis (FEA) was carried out using models that were obtained through three methods: (a) using a fixed Bézier degree for all of the graphite nodule contours, (b) the present methodology, and (c) using a commercial software. The results were compared using the relative error of the equivalent stresses computed by the FEA, where the proposed methodology results were used as a reference. The present paper does not have the aim to define which models are the correct and which are not. However, in this paper, it has been shown that the errors generated in the discretization process should not be ignored when developing geometric models since they can produce relative errors of up to 35.9% when an estimation of the mechanical behavior is carried out.

**Keywords:** genetic algorithm; Bézier curves; ductile cast iron; micro-scale models; discretization errors; digital image processing

## 1. Introduction

Ductile Cast Irons (DCIs) have become one of the most important materials when it is desired to manufacture mechanical components that will be exposed to low to moderate stress with complex and large shapes, due to their low production costs and their excellent castability [1]. DCIs are ferrous alloys that are comprised of graphite elements within a ferritic matrix, where the graphite elements, usually called graphite nodules, are characterized by a semi-spherical shape [2]. Because of the particular geometry of the graphite nodules, the DCIs have good characteristics, such as excellent mechanical properties, machinability characteristics, superior corrosion, and abrasive resistance [3–6]. The different DCIs mechanical properties, such as, high values of tensile strength and Young's modulus, among others [7], are some of the reasons that make DCIs very versatile for different engineering fields such as the automotive industry, mining industry, among others [8,9]. To perform the analysis of the mechanical properties, it is necessary to use computational tools, such as the Finite Element Analysis (FEA), which allows for relating the mechanical behavior with the microstructural properties of the DCI [10,11]. In order to obtain adequate results through the FEA, it is necessary to develop models that represent the geometry of the DCI as closely as possible to the real geometries (or to that established

by studies concerning nodule sphericity), since models with incorrect approximations, which can show very pronounced or irregular graphite nodules contours, can generate stress concentrators that will lead in practice to an incorrect estimation of the mechanical properties in the FEA simulation. Therefore, it is very important to generate methodologies that allow for obtaining the micro-scale models with the appropriate geometry without losing the sphericity that conceptually defines the DCIs.

According to the models that have been generated to represent the DCI microstructure, two types can be identified, those who completely idealize the microstructure, and those that try to fit to the real geometry of the DCIs. Among the works that have idealized the models is the work of Rodríguez et al. [12], where two-dimensional and three-dimensional multi-particle cell models were employed to obtain the Young's modulus and the Poisson's ratio of a DCI using a FEA. The cells were modeled assuming that the matrix was homogeneous and that the nodules were considered perfectly spherical or circular holes for the two-dimensional cells. Based on this consideration, several works have studied the effects that the consideration of graphite nodules as holes on the mechanical properties values can have. For example, the work of Di Cocco et al. [13] proposed a methodology by means of image processing to develop a three-dimensional (3D) microstructural model in order to implement a FEA for analyzing the stress distribution. They used models where the microstructure was considered as biphasic, and models with the nodules that were considered as holes, and demonstrated that it is not possible to consider graphite nodules as holes, because in addition to being unrealistic, such considerations decrease the intensification of the stress near of the graphite nodules. In the same sense, there is the work of Kasvayee et al. [14] which studied the distribution of strains produced in a tensile test of a DCI; in their work, as Di Cocco does, demonstrated that the assumption of graphite nodules as holes in the microstructure is not valid, since taking into account this consideration occurred high deformations around all of the graphite nodules, unlike when the nodules are considered as solids, where the deformations were only located on some specific nodules. Therefore, the models that consider graphite nodules as holes, despite the effects on the mechanical properties of graphite in the microstructure of DCIs. On the other hand, other works have used models where the graphite nodules are not considered as holes, but as ideal spheres of graphite, with the aim of making a thermoelastic formulation of the internal structure of graphite nodules to verify the elastic behavior of a DCI by means of an FEA [10]. At this point, the works that are mentioned above have only used geometric models where nodules are considered as holes or ideal spheres. To represent how spherical graphite nodules are within a DCI, there is an index called *Circular Shape Factor (CSF)*, it has been shown that graphite nodules within a DCI have a *CSF* value that varies between 0.9 and 1 [15], where a value of 1 would represent a completely spherical nodule or in two dimensions a perfect circle. Therefore, all of the works that have used idealized models have considered their nodules or holes with a *CSF* value of 1, such consideration is impossible in the real morphologies, and also, as already mentioned, has significant effects on the mechanical behavior.

On the other hand, there are the works that have developed models that try to fit or approach to the real geometry of the DCIs. For instance, the work of Carazo et al. [11], where they predicted Young's effective modulus and Poisson's ratio of a DCI based on a multi-scale computational model. The models were generated using image processing techniques to extract the coordinates of the pixels representing the graphite nodules contours, which are used to generate the model for the FEA. They considered a node within each pixel of the contour and then joined each node using straight lines. In this context, there is the work of Kasvayee et al. [14], which studied the distribution of strains that were produced in a tensile test of a DCI, when comparing finite element simulation and measurements by digital image correlation, in their work they used real micrographs to produce their models. Another work is that of Fernandino et al. [16], in which it was developed a methodology for predicting the elastic behavior of a DCI using multi-scale analysis. The procedure combines computational techniques for FEA, micrographic analysis to generate FEA models, and micro-indentation tests to identify the elastic behavior of the different phases of the microstructure. The geometric models were generated employing image processing tools to segment the nodules; the model is estimated by considering

a square matrix with square elements whose resolution was 1  $\mu\text{m}$ , in order to approach the DCIs geometry accurately. However, when the model is represented by square elements, the nodules contours are affected, which also is not realistic. In the methodologies that are followed by the previous works, the image processing is used to extract the graphite nodules contours conserving geometries that are more similar to the real models in comparison with the ideal models, however, when image processing techniques are applied, an error occurs in the extracted contours due to the discretization process at the pixel level, which can affect the real geometry of the DCI. In this sense, it is demonstrated that the variability in the geometry of the generated models has a significant effect on the values of the mechanical properties that were estimated by the application of a FEA, as demonstrated by the works of Carvalho et al. [17] and Ahmadi et al. [18]. Therefore, it has been concluded, from the various works, that the need to generate geometric models closer to reality, since according to the methodology that was used to generate the models it is possible to obtain different variations in the geometries of the modeled material, and hence a variation in the estimated mechanical properties. As shown in previous works, image processing has been used to obtain realistic models, however, the problem lies at the moment of interpolating to generate the contours of the nodules, and so far, only simple and linear approximations have been reported. Therefore, it would be ideal to apply other methods of curves interpolation, for instance, Bézier curves, and some algorithm of optimization for the generation of the curves, since they have been appropriate in other applications [19–21].

The present work proposes a methodology that is capable of generating geometric microscale-models of the microstructure of a DCI; the generated geometric models preserves the smoothness of graphite nodules contours that are lost by discretization errors when extracting the contours using image processing techniques. The methodology is based on the extraction of the geometric data from a micrographical image of a DCI; after that, the obtained data is processed to obtain an approximation through Bézier curves using an optimization method based on genetic algorithms (GA) with the aim of determining the optimal degree of the Bézier curve to approximate the contour of each graphite nodule, and thus to obtain a model that best approximates to the DCI original geometry. The validation of the proposed methodology is done through an experimental comparison with the models obtained using a fixed Bézier curve degree for all of the graphite nodules and a model obtained with commercial software. The comparison is carried out using an FEA to demonstrate the effect on the mechanical properties of variations in the geometry of different models of a DCI.

## 2. Background

### 2.1. Discretization Error Due to Image Processing

The geometric micro-scale-models play an important function when a FEA is performed with the objective to estimate the mechanical behavior. The microscale-models are usually obtained from the nodules contours of a DCI micrograph (Figure 1a) using image processing techniques, as shown in Figure 1b, and from this data, the geometric models are generated, as it can be observed in Figure 1c, in this figure the model was generated using commercial software called img2CAD (Img2CAD LLC., Cologne, Germany). As it can be seen in Figure 1c, some regions of the contour of the model are completely straight due to the contour that is computed at the pixel level; besides, other sections have corners with angles of  $45^\circ$  and  $90^\circ$ , which can produce stress concentrators in a FEA. Furthermore, these sections do not represent the geometric characteristics of graphite nodules, since a DCI is characterized by the semi-sphericity of its graphite nodules, as they have a CSF value of between 0.9 and 1 [15]. These geometric characteristics are a part of the errors that are produced by the discretization at the pixel level at the time of obtaining the contours through image processing. Although the geometric variations may be too small to observe, they have an effect on the estimation of the mechanical properties in a FEA using the models obtained. Therefore, new alternatives are required to create methodologies capable of generating models, which reduce the possible errors due to geometric discretization.

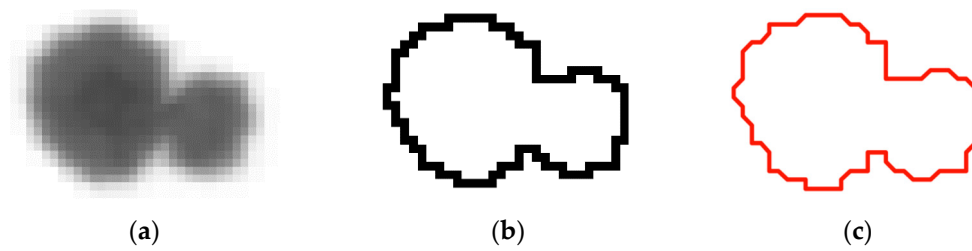


**Figure 1.** (a) Original micrography; (b) Contour obtained using image processing; (c) Model using commercial img2CAD software.

### 2.2. Bézier Curves

The Bézier curves have been used to generate smooth trajectories, so they can be considered for the approximation of the points that form the graphite nodules contours, as they have a semi-spherical morphology. Once the coordinates of the pixels (points) that compose the graphite nodules contours have been obtained using image processing, the Bezier curves are obtained. To obtain the curves, the contour is divided into two subsets, one superior ( $S_{sup}$ ) and one inferior ( $S_{inf}$ ), and a Bezier curve is obtained for each subset; once the curves are computed, then they are joined to obtain the curve that represents the contour of the complete nodule.

When considering that is necessary to generate a Bézier curve ( $\mathbf{C}(t)$ ) of degree  $n$  for a subset of points,  $\mathbf{A} = \{a_0, a_1, \dots, a_k\}$ , which could be  $S_{sup}$  o  $S_{inf}$ , with a points number of  $(k + 1)$ , it requires to satisfy the following equation for all points:

$$\mathbf{C}(t_j) = \sum_{i=0}^n \mathbf{p} \mathbf{B}_{i,n}(t_j) = a_j \quad \text{for } j = 0, 1, 2, \dots, k \quad (1)$$

where  $\mathbf{B}_{i,n}(t)$  are called the Bernstein polynomials and  $\mathbf{p}$  are the control points. Equation (1) can be rewritten in the next matrix form:

$$\overbrace{\begin{pmatrix} \mathbf{B}_{0,n}(t_0) & \mathbf{B}_{1,n}(t_0) & \mathbf{B}_{2,n}(t_0) & \cdots & \mathbf{B}_{n,n}(t_0) \\ \mathbf{B}_{0,n}(t_1) & \mathbf{B}_{1,n}(t_1) & \mathbf{B}_{2,n}(t_1) & \cdots & \mathbf{B}_{n,n}(t_1) \\ \vdots & \vdots & \vdots & \ddots & \vdots \\ \mathbf{B}_{0,n}(t_k) & \mathbf{B}_{1,n}(t_k) & \mathbf{B}_{2,n}(t_k) & \cdots & \mathbf{B}_{n,n}(t_k) \end{pmatrix}}^{\mathbf{B}} \overbrace{\begin{pmatrix} p_0 \\ p_1 \\ \vdots \\ p_n \end{pmatrix}}^{\mathbf{C}} = \overbrace{\begin{pmatrix} a_0 \\ a_1 \\ \vdots \\ a_k \end{pmatrix}}^{\mathbf{A}} \quad (2)$$

Equation (2) can be summarized as  $\mathbf{BC} = \mathbf{A}$ , where  $\mathbf{B}$  is the matrix of Bernstein's polynomials,  $\mathbf{A}$  is the vector who contains the pixels belonging to the contour of the graphite nodule (they are the points to be approximated by the Bézier curve), and  $\mathbf{C}$  is the vector containing the control points, which are calculated by solving the matrix system in Equation (2). As it can be seen,  $n$  must be equal to  $k$  with the objective to appropriately compute the control points, which basically define the Bézier curve [22].

In the generation of a Bézier curve, one of the most important parameters to select is the Bézier curve degree ( $n$ ), as this parameter defines whether the curve will be more or less smooth. Hence, it is necessary to use an algorithm to optimize the selection of  $n$  according to the particular characteristics of each graphite nodule. In this work, the CSF and the number of points that each subset contains are used as inputs of the optimization algorithm.

### 2.3. Standard Genetic Algorithms-Based Optimization

The Standard Genetic Algorithms (SGA) are powerful meta-heuristic techniques that are used in variables searching and optimization problems [23–26], where the design/searching spaces are characterized by their discontinuity and non-convexity and the presence of mixed continuous-discrete variables. These algorithms, first presented by Holland [27], are philosophically based on Darwin's

principle of survival of the fittest considered as an evolution-based procedure that meets with the natural genetics and natural selection.

The general scheme of the SGA can be observed in Figure 2, which provides the necessary information to implement such scheme:

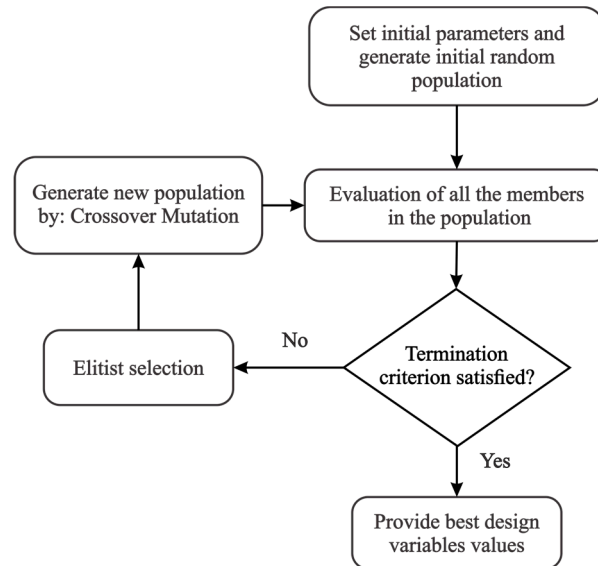


**Figure 2.** General scheme of the Standard Genetic Algorithms (SGA).

The first step consists in specifying all of the initial parameters and generating the initial random population; then, the population must be evaluated using the stopping criterion of the iterative process. If the termination criterion is satisfied, then best design variables values must be provided and the selection of the best individuals must be performed. Once the best individuals are selected, a new population must be generated by applying the genetic operators: crossover and mutation. Finally, this new population replaces the original population, and the iterative process is executed until nominal convergence is reached or stopping criterion is satisfied.

### 3. Methodology

The proposed methodology develops micro-scale models of a DCI, which are then characterized by the moderate smoothness of the graphite nodule contours. In this way, the discretization errors generated when the graphite nodule contours are extracted using image processing techniques are reduced. The methodology is composed of three main stages, which are shown in Figure 3. The first stage extracts the coordinates of the points and the  $CSF_{dig}$  values that are obtained at the digital level ( $CSF_{dig}$ ) of the graphite nodules contours from a DCI micrograph in a Bitmap format (BMP); in the second stage, the coordinates of the points and the  $CSF_{dig}$  values are used to estimate an approximation to a Bézier curve for each graphite nodule contour by selecting the optimal degree,  $n_{opt}$ , for each curve while using genetic algorithms (GA). Finally, the third stage generates the micro-scale model of the DCI microstructure in a drawing exchange format (DXF). Next, each of the stages that compose the methodology will be explained in detail.

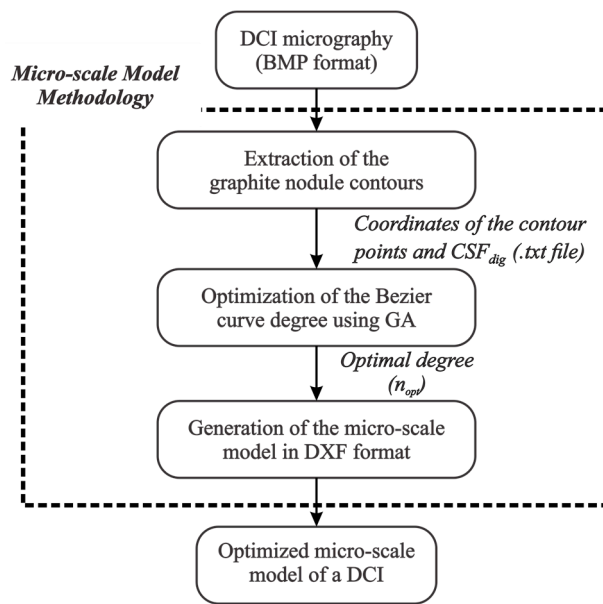


Figure 3. General scheme of the methodology followed.

### 3.1. Extraction of the Graphite Nodule Contours

The objective of this step is to extract the coordinates of the points and the  $CSF_{dig}$  values of the graphite nodules contours from a DCI micrography, and consists in a series of image processing algorithms, such as can be observed in Figure 4. First, a binarization algorithm is applied, employing the Otsu method [13]. Once the image has been binarized, the nodules that are at the edges are removed by reconstruction dilation [28], since these nodules do not have their complete geometry within the micrograph. After that, the graphite nodules smaller than  $3 \mu\text{m}$  are removed through an opening by reconstruction [29], since they are considered to be metallic inclusions or porosities, they can even be either the beginning or the end of a larger nodule, because the micrographs are two-dimensional (2D) representations of the graphite nodules. After the image segmentation, the overlapped nodules are separated, first applying an algorithm called distance function [29] to the binarized image and then the watershed algorithm [30]. Subsequently, a labeling is applied, which consists in assigning a level of gray to each graphite nodule in order to identify each of the graphite nodules. Finally, the whole image is read to identify the pixels (points) that belong to the contours. While the pixels belonging to the contours are identified, their coordinates are stored and grouped into a set depending on the graphite nodule (gray level) to which each pixel corresponds. In this same step, it is obtained the perimeter and the total area corresponding to each graphite nodule, which are required to calculate the  $CSF_{dig}$  [15]. Then, the coordinates of the points and the  $CSF_{dig}$  values of the graphite nodules contours are written in a text file, which is used to carry out the next stage.

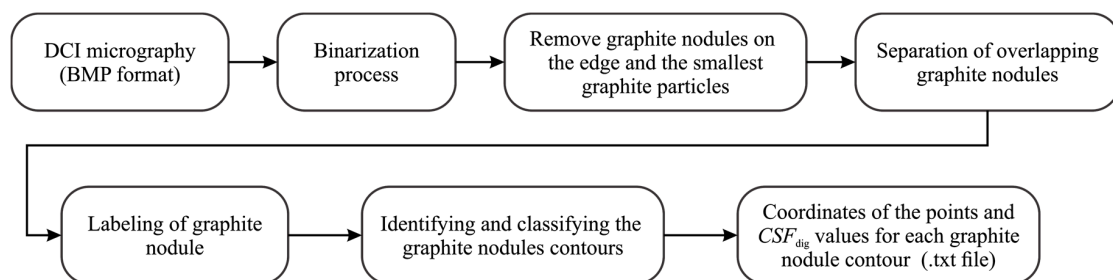


Figure 4. Steps followed to extract the graphite nodule contours.

### 3.2. Optimization of the Bezier Curve Degree Using GA

Once the coordinates of the points and  $CSF_{dig}$  values of the graphite nodule contours are obtained, then these points that are defined by the set  $\mathbf{A} = \{a_0, a_1, a_2, \dots, a_k\}$  with a points number of  $(k + 1)$  must be approximated by some type of curve in order to reduce the errors caused by the discretization process. In this work, it was decided to use approximations by Bézier curves as these generate smooth curves and are currently used in different applications [19,31,32]. However, there is a wide possibility of degrees to be used for generating Bézier curves; therefore, it requires an optimization strategy that simplifies the selection of the optimal degree,  $n_{opt}$ , of the Bézier curve for each of the graphite nodules contours. The optimization algorithm that is used in the present work was implemented in the MATLAB software and is based on genetic algorithms. The diagram of the steps that were followed to implement the optimization method can be seen in Figure 5.

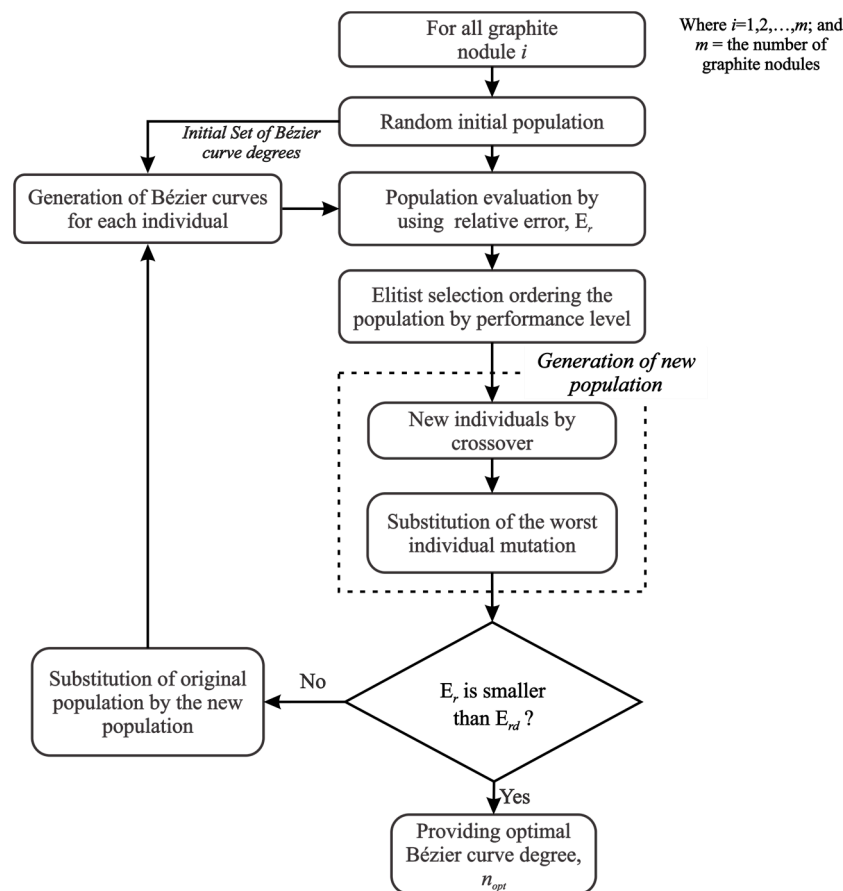


Figure 5. General scheme of the Bézier curves optimization.

First, an initial set (population) containing a given number of different Bézier curves degrees (individuals) is generated, these individuals are selected randomly from a given range of Bézier degrees, where each individual represents a potential solution of the optimal degree of the Bezier curve that best fit the micro-scale model of the nodule  $i$ , which is being analyzed. Then, the Bézier curves are generated for each of the proposed degree in the initial set, and for each individual, the relative error,  $E_r$ , is computed as:

$$E_r = \frac{|CSF_{dig} - CSF_{est}|}{CSF_{dig}} \quad (3)$$

where  $CSF_{dig}$  is the circular shape factor obtained digitally (image processing), and  $CSF_{est}$  is the estimated shape factor for each of the individuals of the Bézier degrees population randomly generated.

The relative error,  $E_r$ , represents the performance of each Bézier degree (fitness of the individual). According to each of the  $E_r$  that are obtained, the initial population is reordered, this corresponds to the elitist selection of the individuals, leaving in the first place the Bézier curve degree whose  $E_r$  is the lowest (best fitness), and lastly the Bézier curve degree with the highest  $E_r$  (worst fitness). Once the degrees with the best performance have been selected, a new population is generated, which will be evaluated in the next iteration of the evolutionary process. The generation of this population will be done by using the cross over operation between the best individuals (those who have the lowest  $E_r$ ), whereas the individuals with the highest  $E_r$  will be replaced using the mutation operator. It should be noted that during the elitist selection, the best degree that is obtained will be kept in the highest position (during re-ordering), and will only be replaced if a degree of curve with a better fit is found in a following iteration. This will guarantee the curve degree evaluation to its optimal value. The algorithm ends when the relative error,  $E_r$ , obtained for the Bézier curve degree at the highest position is less than the termination criterion, which is the desired relative error,  $E_{rd}$ . It is important to mention that the proposed models do not have the aim to converge to the  $CSF_{dig}$  values, because if the proposed curves had the same  $CSF_{dig}$  values, it would be repeating the same errors that were produced by the discretization process, for this reason is that the termination criterion is the  $E_{rd}$  value instead of  $CSF_{dig}$ , which function is to give a tolerance factor to produce smooth curves in the proposed models.

### 3.3. Generation of the Micro-Scale Model in DXF Format

The generation of the micro-scale models consists of writing the Bézier curves in a DXF format file using the coordinates of the points,  $\mathbf{A} = \{a_0, a_1, \dots, a_k\}$ , that compose the graphite nodule contour and the optimal degree,  $n_{opt}$ , found in the previous section. These two components are used to form the matrix system in Equation (2), and the system solution gives directly the control points,  $\mathbf{C} = \{p_0, p_1, \dots, p_n\}$ , which define the Bézier curve. Once the control points have been computed, these points are joined using polylines and the curves are written in a DXF format file, and all this is achieved by using the MATLAB drawing tools provided by the corresponding libraries to draw in a DXF format.

## 4. Results and Discussion

This section presents the results that are obtained from the different stages followed to obtain the DCI micro-scale models. This section is divided into four sections: the first section shows the results of the steps followed with the aim to extract the contours and the computation of the  $CSF_{dig}$  value of the graphite nodules of a DCI microstructure. The second section shows the models that were obtained with the proposed methodology of fourteen selected graphite nodules due to their irregular geometries and their different sizes. The third section makes a comparison of the geometric behavior between the model developed with the proposed methodology, a set of models that are generated obtained with a fixed Bézier curve degree and a model obtained using a commercial software called img2CAD; in this same section, it is analyzed the  $CSF_{est}$  and  $E_r$  values that are obtained for the different models using a fixed Bézier curve degree, to demonstrate the effect that the different degrees on the circularity ( $CSF$ ) of each nodule have; besides, it is also shown that the optimal degree that is chosen by the methodology proposed for four particular nodules. Finally, in the fourth section a validation of the proposed methodology using a FEA of the three types of models that were analyzed is performed with the objective of studying the effect on the equivalent stresses that the different models generate.

### 4.1. Graphite Nodules Contours

Figure 6 shows the results of the different steps that were followed, depicted in Figure 4, for the coordinates extraction of the graphite nodule contours from the DCI original micrograph (Figure 6a). A binarization process was applied to the micrograph of Figure 6a, where an image (Figure 6b) was obtained in white (graphite nodules) and black (ferritic matrix). Subsequently, the nodules at the edges and the smaller particles were removed, as shown in Figure 6c. In this image, a particular

region that is enclosed in a yellow rectangle can be observed, to which a zoom was applied to show a pair of nodules (red and green) that are overlapped, when two nodules are very close in a DCI microstructure, they visually generate overlapping morphologies that could be considered as one, however in the industrial field, there are different works that recommend to separate them [29,33]. For this reason, in Figure 6d, the image shows that the overlapping nodules have been separated (region contained in the blue rectangle). Afterwards, a labeling was applied (Figure 6e), and finally in Figure 6f, the contours that were extracted from the graphite nodules of the original micrograph can be seen. Once the aforementioned procedure is completed, a file in a .txt format is generated. This file contains the number and coordinates of the points that form the graphite nodules contours, as well as the  $CSF_{dig}$  values that were obtained at the image processing level, since these information are necessary to apply the proposed methodology based on genetic algorithms to optimize the selection of the Bézier curves degree that approximate the contours of each one of the obtained nodules at pixel level.

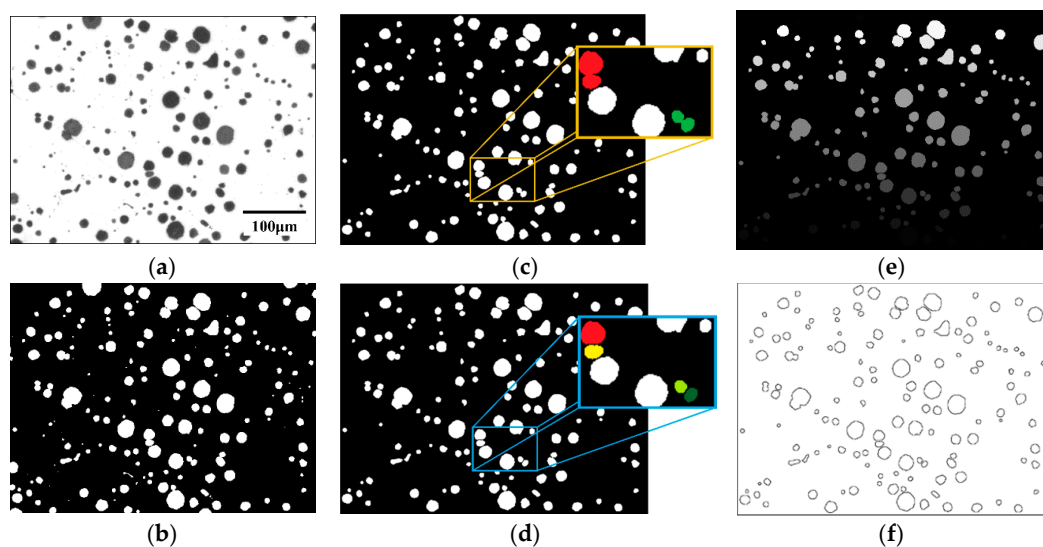


**Figure 6.** (a) Original micrography; (b) Binarized image; (c) Image without the edge nodules nor the smallest nodules; (d) Image with overlapped nodules separated; (e) Labeled image; and, (f) Graphite nodules contours extracted.

#### 4.2. Optimized Micro-Scale Models through Genetic Algorithms

The Bézier curves of fourteen nodules of the models obtained with the proposed methodology are shown in Figure 7. These nodules were chosen due to their irregular shapes and their different sizes, since they are critical geometric shapes that can be found in the microstructure of a DCI. The models were obtained using genetic algorithms to optimize the selection of the Bézier curves degree to represent the graphite nodules contours. For the implementation of the genetic algorithm, it was considered a population with eight individuals (degrees), which were randomly selected in a range of Bézier degrees between 4 and 25. The genetic algorithm chose the Bézier curve degree, which has the relative error that is smaller than the desired relative error, which in this paper has a value of 0.45. Once the optimal Bézier degrees were selected for each graphite nodule, the matrix system in Equation (2) was evaluated in the points to be approximated,  $\mathbf{A} = \{a_0, a_1, a_2, \dots, a_k\}$  and the solution of the system yield the control points,  $\mathbf{C} = \{p_0, p_1, \dots, p_n\}$ . These points define the Bézier curves for each nodule. Once the control points have been obtained, they are joined by polylines and the curves were written in a DXF format file, this was achieved by the MATLAB drawing tools and the corresponding libraries to draw in a DXF format. As can be observed in the nodules of Figure 7, the Bézier curves (red contours) that were obtained by the proposed methodology approach smoothly to the digital

contours (black contours), avoiding the errors that are caused by the discretization process, for example: corners at  $90^\circ$  and the completely flat segments, which can be seen more clearly in the black outlines of the nodules shown in Figure 7.

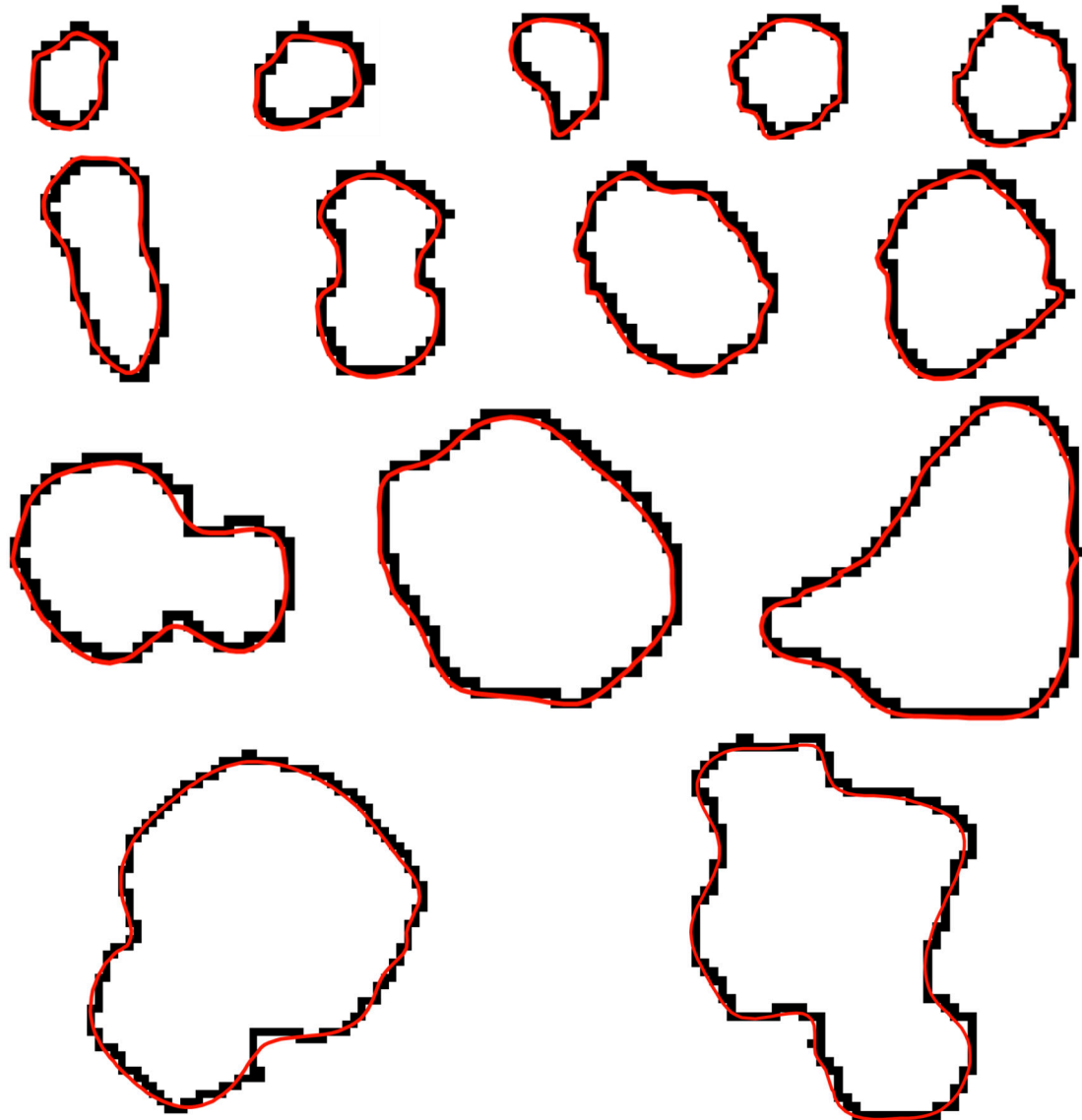


**Figure 7.** Contours of the 14 graphite nodules: at pixel level obtained by image processing (black) and model curves obtained by genetic algorithms (red).

#### 4.3. Geometric Comparison of the Obtained Models

With the objective of analyzing the geometric behavior of the obtained models, a comparison was made between the models that are generated with three methods: (a) using a fixed Bézier degree for all of the graphite nodules; (b) the proposed methodology; and, (c) with a commercial software, img2CAD. There are different works that used this commercial software to generate their models in a CAD format [34,35]. Table 1 shows the models obtained from four nodules (A, B, C and D) using the three different methods mentioned, besides the  $CSF_{est}$  and  $E_r$  values for each graphite nodule are shown, where the maximum errors are highlighted in bold. Regarding the models that are generated using a fixed Bézier degree for all the nodules, three different models were created with the following degrees: 4, 10, and 18.

**Table 1.** Geometric comparison of the obtained models using the three different methods: (a) using a fixed Bézier degree for all the graphite nodules; (b) the proposed methodology; and (c) with a commercial software, img2CAD.

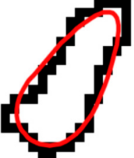
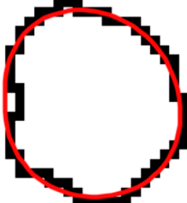
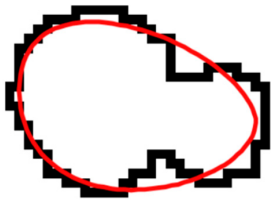
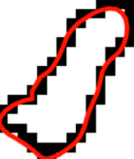
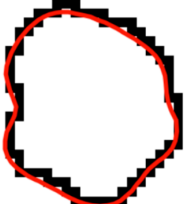
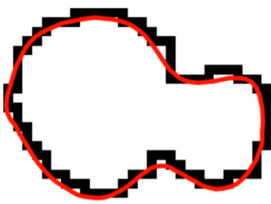
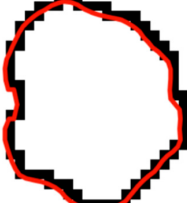
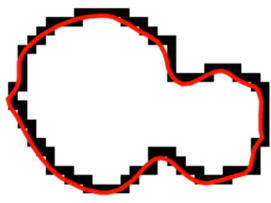
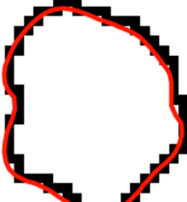
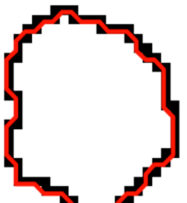
Method	Model	Nodule A	Nodule B	Nodule C	Nodule D
(a)	$n = 4$				
	$CSF_{est}$	0.9911	0.7820	0.9930	0.9260
	$E_r$	0.1203	<b>0.7019</b>	<b>0.5465</b>	<b>0.8376</b>
	$n = 10$				
	$CSF_{est}$	0.8902	0.6239	0.9348	0.7879
	$E_r$	0.0062	0.3578	0.4559	0.5635
	$n = 18$				
	$CSF_{est}$	0.1231	0.5158	0.8858	0.7871
	$E_r$	<b>0.8608</b>	0.1225	0.3796	0.5657
	(b)	GA			
$n_{opt}$		9	13	20	24
$CSF_{est}$		0.9247	0.5764	0.884	0.7275
$E_r$		0.0452	0.2544	0.3769	0.4437
(c)		Img2CAD			
	$CSF_{est}$	0.8532	0.46722	0.6291	0.5020
	$E_r$	0.0354	0.0168	0.0201	0.0037

Table 1 shows the generated models, where geometric evolution it can be seen as the Bézier curve degree increases. In relation to the models obtained using a fixed Bézier curve degree for all of the nodules, it can be seen that the curves that are obtained with Bézier degrees of 4 are curves with high  $CSF_{est}$  values and high  $E_r$  values, therefore do not approximate adequately to the geometry of the

digital contours; on the other hand, as the curve degree increases (degree 10), the curves approximate to the contours obtained digitally preserving the smoothness that characterizes them, unlike the models that are obtained with commercial img2CAD software and the models that are obtained by another methodologies [11,14,16], where no smooth algorithms has been applied.

It can also be observed for the models with a curve degree of 10, that the  $CSF_{est}$  values decrease noticeably as opposed to the  $CSF_{est}$  values that are obtained with degree 4, as a better approximation with respect to the digital contours is obtained. When it is used a degree of 18, depending of the analyzed nodule, geometries with some acute contours are generated (nodule B), which causes the  $CSF_{est}$  value to decrease even more than the obtained ones with a degree of 10 due to the great similarities with the digital contours and the repeatability of geometric errors that are created by the discretization process. Another feature that can be seen is that nodules B, C, and D can be represented with curves degrees of 18 without any problem, unlike smaller nodules like A. This effect can be explained as the system represented in Equation (2) becomes indeterminate as the curve degree used is greater than the number of points that the contour has, generating spurious geometries (blue contour). In this regard, it is seen as a disadvantage of using the same degree for the Bézier curve for all nodules since each nodule has a different number of points in its contour and sometimes a specific degree is not appropriate for other nodule due to its particular characteristics. In contrast, when genetic algorithms are used to optimize the selection of Bézier degree for each graphite nodule, that problem is avoided as can be seen in Table 1, where using GA a curve degree of 9 was set for the nodule A, since this value best approximates the contour, as a higher order for this specific nodule would produce a  $CSF_{est}$  that is too low, which, in consequence, would generate an increased relative error. In this way, a higher degree for this kind of nodule is not considered as a candidate for the GA. Further, using the proposed methodology, each nodule was approximated with optimal Bézier curve degrees that are not too small to obtain exaggeratedly smooth curves, such as degree of 4, which have very large  $CSF_{est}$  and approaches to an idealistic model, but are not too large to fall into curves that simulate errors due to the discretization process, such as degree of 18, where  $CSF_{est}$  decrease significantly.

#### 4.4. Validation Using a FEA

The models that were obtained with the three methods: (a) using a fixed Bezier curve degree (starting with a degree of 4 with increments of 2 up to a degree of 12) for all of the graphite nodules contours; (b) using the proposed methodology; and, (c) using a commercial software (img2CAD), were imported into WORKBENCH from ANSYS© and an extrusion of 10  $\mu\text{m}$  was applied with the aim to perform a FEA in this platform. The geometric models were composed of two phases: graphite nodules and a ferritic matrix. The behavior of both these phases, the ferritic matrix and the graphite, was considered as isotropic. The values of the Young's modulus of the graphite and the ferritic matrix used were 15 GPa and 235 GPa, respectively, and the Poisson ratio of 0.28 for both of the phases [16]. The geometric models were discretized by means of solid tetrahedral elements, which are the basic three-dimensional elements that are used by the abovementioned software, producing a total number of 88658 elements. The models were subjected to an applied loading of 50 mN, which is distributed to the top surface in the positive y-direction with a clamped bottom surface. Based on the obtained results, the concentration of stresses, that is, the maximum stresses of Von-Mises are obtained in the vicinity of the graphite nodules. The model that is obtained with the proposed methodology is shown in Figure 8a. Table 2 shows the maximum stresses and relative errors that are obtained by the FEA for the models developed with the three abovementioned methods. The relative errors ( $E_s$ ) of the stresses were calculated by the following equation:

$$E_s = \frac{\sigma_{ref} - \sigma_e}{\sigma_{ref}} \times 100\% \quad (4)$$

where,  $\sigma_{ref}$ , is the maximum stress obtained with the proposed methodology, whose value is 64 MPa (Figure 8b), and was taking as reference since it is desired to estimate the error (variation)

in the stresses obtained by the other methods in relation to the proposed methodology, and  $\sigma_e$  is the stress computed from other methods.

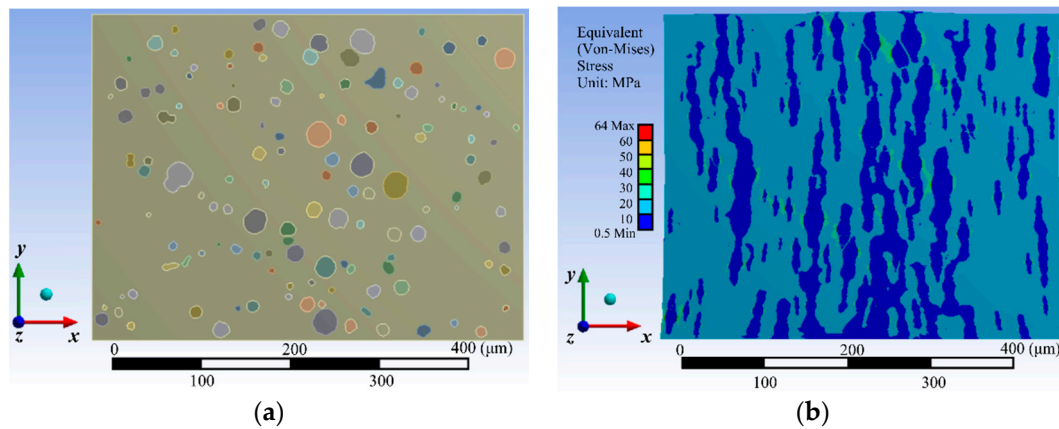


**Figure 8.** (a) Micro-scale model obtained by the proposed methodology from a ductile Cast Irons (DCI) micrograph (Figure 6a); (b) Results from the Finite Element Analysis of the model in Figure 8a.

**Table 2.** Stresses and relative errors obtained by the Finite Element Analysis (FEA) for the different methods used.

Geometric Models		Equivalent Stress (MPa)	Relative Error (%)
Proposed methodology (GA)		64	Ref.
Commercial software (SC)		87	−35.9
Fixed	4	48	25.0
Bézier curve	6	55	14.1
	8	56	12.5
	10	68	−6.3
degree	12	86	−34.4

Based on Table 2, the relative error that is obtained with the commercial software model (CSM) was  $-35.9\%$ . The negative value means that the stress that is produced for the CSM is greater than the reference, as the curves of the graphite nodules contours that are obtained by the CSM have characteristics that reproduce the geometric errors generated in the discretization process. On the other hand, for the models that used a fixed Bézier curve degree, errors of  $25\%$  and up to  $-34.4\%$  were obtained for the Bézier curve degrees of 4 and 12, respectively. In particular, for the model that used a Bézier curve degree of 4, the positive relative error is due to the maximum stress was smaller than the reference since the curves of the graphite nodules contours have values of  $CSF_{est}$  near to the unit, which represents curves with an almost spherical geometry. Therefore, based on the obtained results it is confirmed that the discretization process generates significant errors in the estimation of the stresses produced when a FEA is applied for the micro-scale model of a DCI microstructure, therefore the errors generated in the discretization process should not be ignored when developing geometric models.

## 5. Conclusions

In this work, a methodology that is capable of generating microscale-models of a DCI microstructure is proposed. The models that are generated are characterized by the smoothness in their curves with the objective of avoiding or mitigating the discretization errors produced when the graphite nodules contours are obtained using image processing, since the discretization process by which the graphite nodules contours are obtained, generates significant errors up to  $35.9\%$  in the estimation of the stresses that are produced in a simulation by means of a FEA.

The microscale-models were generated using Bézier curves, where the selection of the degree of the approximated curves for each graphite nodule contour was optimized by means of a genetic

algorithm-based strategy. The selection of the optimal degree was based on the parameters  $CSF_{\text{dig}}$  digitally obtained, the estimated  $CSF_{\text{est}}$  for each curve obtained with the genetic algorithm, and the coordinates of the graphite nodules contours. This advantage is possible to achieve since the GA is capable of deciding which Bézier curve degree is the appropriate according to the characteristics of each nodule.

The commercial software models reproduce the geometric errors that are obtained in the discretization process; this effect can be seen in the obtained values of  $E_r$ , as they have the lowest values compared with the ones obtained using the proposed methodologies. Therefore, the obtained models using the proposed methodology have the advantage, in comparison to the commercial software, that realistic geometries are estimated, thus allows for a reduction of the geometric errors that are generated in the discretization process.

When the graphite nodules are modeled with a very small Bézier curve degree, the generated curves have high  $CSF_{\text{est}}$  values; which, in consequence, produce stresses of low magnitudes. In contrast, as the Bézier curve degree increases, curves are approximated to the contours that are obtained at the digital level, and therefore their  $CSF_{\text{est}}$  decrease noticeably, causing stress concentrators with increased magnitudes of the maximum stresses.

**Acknowledgments:** The first author would like to thank CONACYT for the scholarship (CVU: 419770) given. This publication was funded with CONACYT-PI 243152.

**Author Contributions:** All the authors contributed equally to the present work. J.A.B.-H. performed the analysis of the simulation results, designed genetic algorithm method, analyzed data and wrote the paper; R.A.O.-R. analyzed data and edited the paper; A.Y.J.-C. designed genetic algorithm method and analyzed data; A.D.-G. performed simulation experiments and collected data; L.A.M.-H. designed image processing algorithms, gave technical support and conceptual advice. All authors discussed the results and implications and commented on the manuscript at all stages.

**Conflicts of Interest:** The authors declare no conflict of interest. The founding sponsors had no role in the design of the study; in the collection, analyses, or interpretation of data; in the writing of the manuscript, and in the decision to publish the results.

## References

1. Benedetti, M.; Torresani, E.; Fontanari, V.; Lusuardi, D. Fatigue and Fracture Resistance of Heavy-Section Ferritic Ductile Cast Iron. *Metals* **2017**, *7*, 88. [[CrossRef](#)]
2. Murcia, S.C.; Ossa, E.A.; Celentano, D.J. Nodule Evolution of Ductile Cast Iron during Solidification. *Metall. Mater. Trans. B* **2014**, *45*, 707–718. [[CrossRef](#)]
3. Basso, A.; Caldera, M.; Massone, J. Development of High Silicon Dual Phase Austempered Ductile Iron. *ISIJ Int.* **2015**, *55*, 1106–1113. [[CrossRef](#)]
4. Cardoso, P.H.S.; Israel, C.L.; Strohaecker, T.R. Abrasive wear in Austempered Ductile Irons: A comparison with white cast irons. *Wear* **2014**, *313*, 29–33. [[CrossRef](#)]
5. Han, C.F.; Wang, Q.Q.; Sun, Y.F.; Li, J. Effects of Molybdenum on the Wear Resistance and Corrosion Resistance of Carbide Austempered Ductile Iron. *Metallogr. Microsc. Anal.* **2015**, *4*, 298–304. [[CrossRef](#)]
6. Zhao, P.; Wang, J.; Hang, B.; Wang, Y.; Ma, J.; Zhao, X.; Wang, C. Effect of Quenching and Partitioning Heat Treatment on Ductile Cast Irons. In Proceedings of the International Symposium on Materials Application and Engineering, Chiang Mai, Thailand, 20–21 August 2016; Jawaid, M., Kenawy, E.-R., Eds.
7. Fragassa, C.; Pavlovic, A. Compacted and Spheroidal graphite irons: Experimental evaluation of Poisson's ratio. *FME Transl.* **2016**, *44*, 327–332. [[CrossRef](#)]
8. Čanžar, P.; Tonković, Z.; Kodvanj, J. Microstructure influence on fatigue behaviour of nodular cast iron. *Mater. Sci. Eng. A* **2012**, *556*, 88–99. [[CrossRef](#)]
9. Tiedje, N.S. Solidification, processing and properties of ductile cast iron. *Mater. Sci. Technol.* **2010**, *26*, 505–514. [[CrossRef](#)]
10. Andriollo, T.; Thorborg, J.; Tiedje, N.; Hattel, J. A micro-mechanical analysis of thermo-elastic properties and local residual stresses in ductile iron based on a new anisotropic model for the graphite nodules. *Model. Simul. Mater. Sci. Eng.* **2016**, *24*, 55012–55030. [[CrossRef](#)]

11. Carazo, F.D.; Giusti, S.M.; Boccardo, A.D. Effective properties of nodular cast-iron: A multi-scale computational approach. *Comput. Mater. Sci.* **2014**, *82*, 378–390. [[CrossRef](#)]
12. Rodríguez, F.J.; Dardati, P.M.; Godoy, L.A.; Celentano, D.J. Evaluación de propiedades elásticas de la fundición nodular empleando micromecánica computacional. *Revista Internacional de Métodos Numéricos para Cálculo y Diseño en Ingeniería* **2015**, *31*, 91–105. [[CrossRef](#)]
13. Di Cocco, V.; Iacoviello, D.; Iacoviello, F. Graphite nodules influence on DCIs mechanical properties: Experimental and numerical investigation. In Proceedings of the XXIII Italian Group of Fracture Meeting, Favignana, Italy, 22–24 June 2015; Iacoviello, F., Ferro, G.A., Susmel, L., Eds.; pp. 135–143.
14. Kasvayee, K.A.; Salomonsson, K.; Ghassemali, E.; Jarfors, A.E. Microstructural strain distribution in ductile iron; comparison between finite element simulation and digital image correlation measurements. *Mater. Sci. Eng. A* **2016**, *655*, 27–35. [[CrossRef](#)]
15. Vaško, A. Evaluation of Shape of Graphite Particles in Cast Irons by a Shape Factor. In Proceedings of the 32nd DANUBIA ADRIA Symposium on Advanced in Experimental Mechanics, Žilina, Slovakia, 22–25 September 2016; Nicoletto, G., Pastrama, S.D., Emri, I., Eds.; Volume 3, pp. 1199–1204.
16. Fernandino, D.O.; Csilino, A.P.; Boeri, R.E. Determination of effective elastic properties of ferritic ductile cast iron by computational homogenization, micrographs and microindentation tests. *Mech. Mater.* **2015**, *83*, 110–121. [[CrossRef](#)]
17. Carvalho, A.; Silva, T.; Loja, M.A.R.; Damásio, F.R. Assessing the influence of material and geometrical uncertainty on the mechanical behavior of functionally graded material plates. *Mech. Adv. Mater. Struct.* **2017**, *24*, 417–426. [[CrossRef](#)]
18. Ahmadi, H.; Nejad, A.Z. Geometrical effects on the local joint flexibility of two-planar tubular DK-joints in jacket substructure of offshore wind turbines under OPB loading. *Thin-Walled Struct.* **2017**, *114*, 122–133. [[CrossRef](#)]
19. Ceruti, A.; Marzocca, P. Heuristic optimization of Bezier curves based trajectories for unconventional airships docking. *Aircr. Eng. Aerosp. Technol.* **2017**, *89*, 76–86. [[CrossRef](#)]
20. Hassan, A.; Abomoharam, M. Modeling and design optimization of a robot gripper mechanism. *Robot. Comput.-Integr. Manuf.* **2017**, *46*, 94–103. [[CrossRef](#)]
21. Kouchmeshky, B.; Zabaras, N. Microstructure model reduction and uncertainty quantification in multiscale deformation processes. *Comput. Mater. Sci.* **2010**, *48*, 213–227. [[CrossRef](#)]
22. Pal, S.; Ganguly, P.; Biswas, P.K. Cubic Bézier approximation of a digitized curve. *Pattern Recognit.* **2007**, *40*, 2730–2741. [[CrossRef](#)]
23. Luo, Z.; LiWang, M.; Lin, Z.; Huang, L.; Du, X.; Guizani, M. Energy-Efficient Caching for Mobile Edge Computing in 5G Networks. *Appl. Sci.* **2017**, *7*, 557. [[CrossRef](#)]
24. Morino, S.; Takahashi, M. Estimating Co-Contraction Activation of Trunk Muscles Using a Novel Musculoskeletal Model for Pregnant Women. *Appl. Sci.* **2017**, *7*, 1067. [[CrossRef](#)]
25. Mohanty, D.; Chandra, A.; Chakraborti, N. Genetic algorithms based multi-objective optimization of an iron making rotary kiln. *Comput. Mater. Sci.* **2009**, *45*, 181–188. [[CrossRef](#)]
26. Dugan, N.; Erkoç, Ş. Genetic algorithm–Monte Carlo hybrid geometry optimization method for atomic clusters. *Comput. Mater. Sci.* **2009**, *45*, 127–132. [[CrossRef](#)]
27. Holland, J.H. *Adaptation in Natural and Artificial Systems: An Introductory Analysis with Applications to Biology, Control, and Artificial Intelligence*; The MIT Press: Cambridge, UK, 1992.
28. Soille, P. *Morphological Image Analysis: Principles and Applications*, 2nd ed.; Springer: Berlin/Heidelberg, Germany, 2004.
29. Morales-Hernández, L.A.; Terol-Villalobos, I.R.; Domínguez-González, A.; Manriquez-Guerrero, F.; Herrera-Ruiz, G. Spatial distribution and spheroidicity characterization of graphite nodules based on morphological tools. *J. Mater. Process. Technol.* **2010**, *210*, 335–342. [[CrossRef](#)]
30. Talbot, H.; Terol-Villalobos, I.R. Binary image segmentation using weighted skeletons. In Proceedings of the Image Algebra and Morphological Image Processing III, San Diego, CA, USA, June 1992; pp. 393–404.
31. Simba, K.R.; Uchiyama, N.; Aldibaja, M.; Sano, S. Vision-based smooth obstacle avoidance motion trajectory generation for autonomous mobile robots using Bézier curves. *Proc. Inst. Mech. Eng. C J. Mech. Eng. Sci.* **2017**, *231*, 541–554. [[CrossRef](#)]
32. Luo, Z.; Wang, Q.; Fan, X.; Gao, Y.; Shui, P. Generalized rational Bézier curves for the rigid body motion design. *Vis. Comput.* **2016**, *32*, 1071–1084. [[CrossRef](#)]

33. Reboucas, E.S.; Braga, A.M.; Marques, R.C.; Reboucas Filho, P.P. A new approach to calculate the nodule density of ductile cast iron graphite using a Level Set. *Measurement* **2016**, *89*, 316–321. [[CrossRef](#)]
34. Philippine, M.A.; Sigmund, O.; Rebeiz, G.M.; Kenny, T.W. Topology optimization of stressed capacitive RF MEMS switches. *J. Microelectron. Syst.* **2013**, *22*, 206–215. [[CrossRef](#)]
35. Sabzevari, M.; Teymoori, R.J.; Sajjadi, S.A. FE modeling of the compressive behavior of porous copper-matrix nanocomposites. *Mater. Des.* **2015**, *86*, 178–183. [[CrossRef](#)]



© 2017 by the authors. Licensee MDPI, Basel, Switzerland. This article is an open access article distributed under the terms and conditions of the Creative Commons Attribution (CC BY) license (<http://creativecommons.org/licenses/by/4.0/>).